PHYSICAL REVIEW B VOLUME 62, NUMBER 16 15 OCTOBER 2000-II

Band-gap modifications of β-FeSi$_2$ with lattice distortions corresponding to the epitaxial relationships on Si(111)

D. B. Migas and Leo Miglio
INFM and Dipartimento di Scienza dei Materiali, Università di Milano "Bicocca," via Cozzi 53, 20125 Milano, Italy

(Received 7 February 2000; revised manuscript received 24 May 2000)

Electronic bands nearby the gap for several strained structures corresponding to the epitaxial relationships of β-FeSi$_2$ on Si(111) have been calculated by first-principles density-functional method. We have also estimated the related elastic energies, where optimization in the strained structures has been allowed for lattice parameters and for atomic positions. Only one of the heavily strained structures corresponding to β-FeSi$_2$(101) and (110)//Si(111), still the most frequently occurring structures in both epitaxial layers and precipitates, displays a sizable change in gap nature. We show that this issue can be interpreted by the unexpected anisotropic behavior of the band gap for uniaxial lattice distortions along the *b* and *c* sides, which are actually very close in size.

I. INTRODUCTION

Among semiconducting silicides, β-FeSi$_2$ recently attracted much attention because of possible applications in optoelectronic and thermoelectric silicon-compatible devices (for a recent review, see Ref. 1). Experimental study showed that this compound displays a direct band gap of 0.84–0.87 eV (Ref. 2) at room temperature, which is within the absorption minimum of optical fibers. Moreover, a light emitting diode by β-FeSi$_2$ precipitates in silicon, operating at 1.5 μm in the low-temperature range, was successfully fabricated by Leong *et al.*[3] However, there are both experimental and theoretical indications that this emission is due to an indirect transition,[4] some tens of meV lower than the direct one.[5] Several calculations of electronic properties in bulk β-FeSi$_2$ were performed by different methods: linear muffin-tin orbitals (LMTO),[6–10] augmented spherical waves,[11] pseudopotentials,[12,13] and full-potential linear augmented plane waves.[13,14] All of them are in the density functional scheme, using the local-density approximation (LDA) or the generalized gradient approximation (GGA) for exchange and correlation: at lattice parameters corresponding to the experimental structure[15] (either optimized or not), the gap estimations range between 0.44 and 0.80 eV, and the positions of the direct and indirect transitions in the Brillouin zone vary with the calculation method, as due to the flat nature of the *d*-like bands nearby the gap (see Fig. 1). Still, most of these calculations agree in indicating the direct transition to be a few tens of meV larger than the indirect one (see details in Refs. 10 and 13).

Despite the difference in the crystal symmetry between iron disilicide (orthorhombic, the *Cmca* space group, $a = 9.863$ Å, $b = 7.791$ Å, and $c = 7.833$ Å)[15] and silicon (cubic $a = 5.431$ Å), epitaxial layers of β-FeSi$_2$ on both Si(001) and Si(111) have been grown in the recent past by a variety of techniques.[1] Still, defects and rotational domains were present, particularly evident in the case of large-scale epitaxial samples. In fact, the *b* and *c* sides are very close in size, and both on square Si(001) and hexagonal Si(111) rotational domains are produced. Moreover, the large lattice misfit for some epitaxial relationships on Si(111) generates misfit dislocations in the film. The most promising results were achieved in precipitates[3,4] at the nanoscale, where the small size of the crystallites could allow for a coherent growth in silicon. The first attempts to estimate the changes in the electronic properties of β-FeSi$_2$ with lattice distortion due to fitting the lattice constants of iron disilicide to the silicon substrates were independently done by LMTO (Miglio and Meregalli[9]) and pseudopotential (Clark *et al.*[12]) calculations. They both found that band dispersion near the gap and the size of the gap for the strained structures, as produced by a few configurations in the epitaxial relationship β-FeSi$_2$(100)//Si(001), are highly sensitive to shrinkage and expansion of both the *b* and *c* sides. However, no real change in the gap nature was observed for this configuration. Therefore, a preliminary study by LMTO was made for β-FeSi$_2$(101) and (110)//Si(111),[10] where the hexagonal symmetry of the silicon substrate requires an opposite uniaxial strain in the *b* and *c* sides (see Fig. 2). It was found that

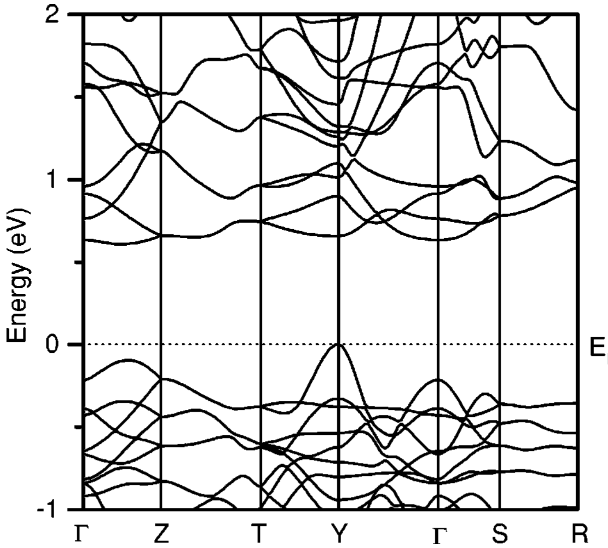

FIG. 1. Band structure of a β-FeSi$_2$ single crystal with fully relaxed structural parameters: configuration $\tilde{B}$ in Table II.

0163-1829/2000/62(16)/11063(8)/$15.00

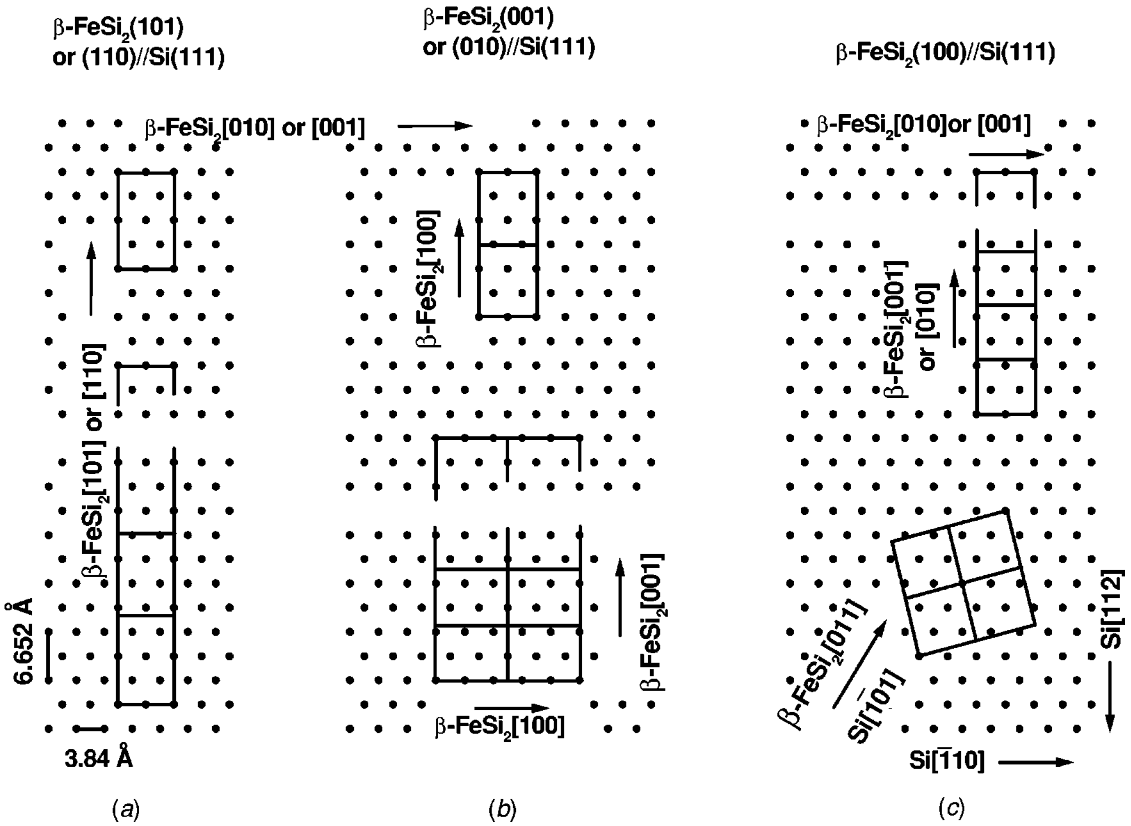

FIG. 2. Top view of the epitaxial relationships for β-FeSi$_2$ on Si(111): (a) β-FeSi$_2$(101) or (110)//Si(111) coherent (top) and commensurate (bottom) interfaces; (b) β-FeSi$_2$(010)//Si(111) or β-FeSi$_2$(001)//Si(111) (top) and β-FeSi$_2$(010)//Si(111) (bottom); (c) β-FeSi$_2$(100)//Si(111) one commensurate interface (top) and one coherent interface orientation (bottom).

the two relationships had rather different gap shapes, one of them displaying a direct gap nature, as provided by the lowering of the first conduction band at Y (see Fig. 1). However, this result was obtained by a computational method which is not suitable for band-structure calculations of strained structures, because no optimization of the lattice constants and relaxation of the atomic positions can be performed.

One goal of this paper is to amend this deficiency, by using a pseudopotential method, which is suited for total-energy calculation and full structural optimization.[13] Another is to expand the analysis on the nature of the band gap for β-FeSi$_2$ on Si(111) by taking into consideration other possible distortions of the crystal structure, according to experimental epitaxial orientations (both in films and precipitates). Finally, as the different gap behavior of the two very similar distortions analyzed in Ref. 9 is produced by an interchange in *b* and *c* shrinkage and expansion, we carry out a systematic study of the gaps with an uniaxial strain of the lattice constants, revealing that a sizable anisotropy is present.

II. MODELS OF β-FeSi$_2$//Si(111) INTERFACES

According to experimental data, there are several orientational relationships for the epitaxial β-FeSi$_2$ layers and precipitates vs Si(111), which are presented in Table I. The most common epitaxy for iron disilicide prepared by solid phase epitaxy (SPE),[16–20] reactive deposition epitaxy,[18,20,21] molecular-beam epitaxy (MBE),[22,23] and ion-beam synthesis[24,25] (IBS) is β-FeSi$_2$(101) or (110)//Si(111). It is difficult to distinguish between the two possible variants, due to the fact that the *b* and *c* sides are nearly equal. However, several experimental studies performed by x-ray[18] and electron-diffraction[21,26] measurements indicated a preferential β-FeSi$_2$(110) epitaxy in some cases, whereas investigations by scanning tunneling microscopy (STM)[17,23] clearly showed the presence only of β-FeSi$_2$(101) in other cases. Some authors believed that this discrepancy could stem from different preparation methods,[18,21] but it is certainly interesting to estimate if a sizable difference in elastic energy would be produced for the two orientations. For such relationships [schematically shown in Fig. 2(a), top side] the diagonal of the *a* side with one of the short *b* or *c* sides (12.569 and 12.595 Å , respectively) is fitted to 13.303 Å (the double of the interatomic distance along Si[112]) and the other short side is set to 7.68 Å (the double of the interatomic distance along Si[$\bar{1}$10]). In this case the diagonal is expanded by 5.3% and 5.5%, whereas the short side is compressed by 1.4% and 2% for β-FeSi$_2$(101)//Si(111) and β-FeSi$_2$(110)//Si(111), respectively. Since such a large lattice mismatch is likely to provide a huge elastic energy, it is also worthwhile to look for commensurate, partially relaxed interfaces. By taking into consideration eight β-FeSi$_2$ interface unit cells along Si[112] it is possible to have +0.8% and +1% misfits instead of -5.3% and -5.5%, respectively [see Fig. 2(a), bottom side]. In such a case the bulk diagonal has to be fitted to 12.472 Å in place of 13.303 Å .

Next possible variants are β-FeSi$_2$(010)//Si(111), with β-FeSi$_2$[001]//Si$\langle\bar{1}10\rangle$, observed for samples obtained by

TABLE I. Some experimental relationships for β-FeSi$_2$ epitaxial layers and precipitates on Si(111).

Epitaxial relationships and azimuthal orientations	Label	Preparation method Epitaxial layers	 Ion beam synthesis	references
β-FeSi$_2$(101)//Si(111) with β-FeSi$_2$[010]// Si$\langle\bar{1}10\rangle$	$E(101), C(101)$	yes	yes	16–26
β-FeSi$_2$(110)//Si(111) with β-FeSi$_2$[001]// Si$\langle\bar{1}10\rangle$	$E(110), C(110)$	yes	yes	16–26
β-FeSi$_2$(010)//Si(111) with β-FeSi$_2$[001]// Si$\langle\bar{1}10\rangle$	$E(010)$		yes	27
β-FeSi$_2$(010)//Si(111) with β-FeSi$_2$[100]// Si$\langle\bar{1}10\rangle$	$E(010)'$		yes	27
β-FeSi$_2$(001)//Si(111) with β-FeSi$_2$[100]// Si$\langle 112\rangle$	$E(001)$	yes		23
β-FeSi$_2$(100)//Si(111) with β-FeSi$_2$[001]// Si$\langle\bar{1}10\rangle$	$E(100)'$	yes		22,23
β-FeSi$_2$(100)//Si(111) with β-FeSi$_2$[010]// Si$\langle\bar{1}10\rangle$	$E(100)$	yes		22,23
β-FeSi$_2$(100)//Si(111) with β-FeSi$_2$[011]// Si$\langle\bar{1}10\rangle$	$C(100)''$	yes		22
β-FeSi$_2$(100)//Si(111) with β-FeSi$_2$[012]// Si$[\bar{1}10]$	$C(100)'''$		yes	4

IBS (Ref. 27) and β-FeSi$_2$(001)//Si(111) with β-FeSi$_2$[010]//Si$\langle\bar{1}10\rangle$ grown by MBE,[23] which are reported in Fig. 2(b), top side. As for the situation described above, here the *b* or *c* side of iron disilicide has to be kept equal to 7.68 Å, but the longest *a* side is set to 9.977 Å. Such a configuration requires a doubling of the periodicity along *a*, which formally corresponds to the interface unit cell $2a \times b$ or $2a\times c$, providing a misfit for *a* as large as -1.1%. One other azimuthal orientation, namely β-FeSi$_2$[100]//Si$\langle\bar{1}10\rangle$, was also found for the (010) epitaxy.[27] This variant is shown in Fig. 2(b), bottom side, where the interface unit cell ($2a\times 6c$, with $a=9.60$ Å, and $c=7.723$ Å) is characterized by misfits of +2.7% and +1.4% for *a* and *c*, respectively.

Several azimuthal orientations for β-FeSi$_2$(100)//Si(111) were reported in literature. One is β-FeSi$_2$[010] or [001]//Si$[\bar{1}10]$, as observed in samples grown by MBE.[21,22] One possible interface unit mesh $5b\times c$ ($5c\times b$) displays a misfit of +1.4% (+2.0%) along Si$\langle\bar{1}10\rangle$ and any of -1.9% (-2.4%) along Si$\langle 112\rangle$.[22] One other possibility is to take $6b\times c$ and $6c\times b$, where the mismatches along Si$\langle 112\rangle$ become much less: +0.4% and +0.9% for *b* and *c*, respectively [see Fig. 2(c), top side]. Another orientation reported in Ref. 22 is β-FeSi$_2$[011]//Si$[\bar{1}10]$. This requires extending the *b* and *c* sides by 4.1% in order to fit the diagonal of *b* and *c* to 11.52 Å . This variant is presented in Fig. 2(c), bottom side. Very recently, a transmission electron microscopy analysis of β-FeSi$_2$ precipitates obtained by ion implantation in silicon also revealed a systematic appearance of nanometric spheres with epitaxial relationship β-FeSi$_2$[012]//Si$[\bar{1}10]$.[4] The lattice parameters of this rather strained crystal structure were estimated to be $a=10.36$ Å, $b=7.36$ Å, and $c=7.40$ Å, corresponding to a misfit of -4.8% for *a* and of +5.5% for the *b* and *c* sides. Misfits as large as 4–5% give rise to large strain energy and to misfit dislocations; however it is interesting to analyze such configurations in a view of possible occurrence in a nanometric structure, as it is the case of Ge on Si(001) where lattice mismatch is about 4%.

III. COMPUTATIONAL METHOD

Calculations of the electronic structure for each β-FeSi$_2$ configuration were performed by the *ab-initio* total energy code VASP 4.4 (Viena *ab initio* simulation package), with a plane-wave basis set and ultrasoft pseudopotentials. This code was described in detail elsewhere.[28] In our study we used the GGA of Perdew and Wang[29] because it predicted the lattice parameters of β-FeSi$_2$ to be very close to the experimental ones.[12,13] Still, both the LDA and GGA give the same shape of the top of the valence band and the bottom of the conduction band, with almost equal energy gaps.[13] Ultrasoft Vanderbilt-type pseudopotentials[30] have been employed for the $3d^7$, $4s^1$ and $3s^2$, $3p^2$ atomic configurations of Fe and Si, respectively. Nonlocal contributions were evaluated using the reciprocal projection scheme. We applied the linear tetrahedron method with Blöchl corrections[31] for a Brillouin-zone integration on a grid of Monkhorst-Pack points.[32] Total-energy minimization was obtained by calculating the Hellmann-Feynman forces and the stress tensor, including the Pulay correction in order to compensate for changes of the basis set due to variation in the shape of the unit cell. In optimizing the lattice parameters and relaxing the atomic positions, the conjugate gradient method has been used. We found that the convergence in the total energy of the unit cell (24 atoms) was better than 0.003 eV using a energy cutoff of 350 eV and a $4\times4\times4$ set of Brillouin-zone points. The plots of the band structures, obtained by the self-consistent charge densities, have been performed with 30 *k*-points along high-symmetry directions of the Brillouin-zone.

IV. RESULTS AND DISCUSSION

A. Structural optimization and elastic energies

We have carried out both atomic position relaxation and lattice parameter optimization for any deformation of the β-FeSi$_2$ structure corresponding to constraints imposed by epitaxial relationships. For the sake of comparison to the bulk electronic structure, we performed a total-energy minimization in the framework of one orthorhombic cell, preserving the *Cmca* symmetry. Thus, we optimized *a* and *b* for β-FeSi$_2$(110)//Si(111); *a* and *c* for β-FeSi$_2$(101)//Si(111); and *a*, *b*, or *c* for β-FeSi$_2$(100), (010) or (001)//Si(111), respectively. The resulting lattice constants and elastic energies are summarized in Table II, where *C* and *E* label coherent and commensurate (i.e., extended) interface unit cells,

TABLE II. Calculated lattice constants (Å) and elastic energy ΔE_{el} (eV/$f.u.$) for several β-FeSi$_2$ configurations. B, E, and C stand for bulk structure, commensurate (i.e., extended), and coherent interface unit cells, respectively; $'$ indicates different orientations on the surface plane (see the text and Table I).

	B	$\overline{B}$	$\widetilde{B}$	$E(101)$	$E(110)$	$E(100)$	$E(100)'$
a	9.863	9.863	9.899	9.74	9.76	9.95	9.96
b	7.791	7.791	7.782	7.68	7.764	7.68	7.76
c	7.833	7.833	7.836	7.789	7.68	7.76	7.68
ΔE_{el}	0.0054	0.0018	0.0000	0.0305	0.0353	0.0141	0.0185
	$E(001)$	$E(010)$	$E(010)'$	$C(100)''$	$C(100)'''$	$C(101)$	$C(110)$
a	9.977	9.977	9.60	9.71	10.36	10.60	10.65
b	7.68	7.82	7.87	8.135	7.36	7.68	7.972
c	7.86	7.68	7.724	8.157	7.40	8.038	7.68
ΔE_{el}	0.0073	0.0163	0.0508	0.1715	0.3501	0.1851	0.2129

respectively (see Table I). The elastic energies (ΔE_{el}) are calculated with respect to the reference structure obtained by a full optimization of the lattice parameters and atomic positions of the bulk configuration ($\widetilde{B}$). The lattice constants of $\widetilde{B}$ (see Table II) are close within the numerical error to the ones obtained by Moroni *et al.*[13] with the same VASP package ($a=9.901$ Å, $b=7.779$ Å, and $c=7.833$ Å), whereas some difference is present with respect to one other pseudopotential calculations by Clark *et al.*[12] ($a=9.825$ Å, $b=7.736$ Å, and $c=7.920$ Å). Just for comparison we have also made calculations of two bulk structures having experimental lattice constants,[15] both with ($\overline{B}$) and without (B) relaxation of the atomic positions. We found that the optimized structures $\widetilde{B}$ and $\overline{B}$ are very close to the experimental one (B), and that the variations in total energy are very small. An interesting feature is that the fractional coordinates of the atomic basis for all the strained structures are practically the same as the ones for B, as a sizable difference can be found in the third or fourth significant figure only [this fact was already found in Ref. 12 for the strained structures β-FeSi$_2$(100)//Si(001)]. This issue proves that, within symmetry constraints, the site stability in each strained case is very close to the one of the experimental bulk structure, as provided by the rather effective Jahn-Teller stabilization.[33]

Estimations of the total energy, presented in Table II, show that β-FeSi$_2$(101) and (110) configurations are very expensive, the largest ones, but that the $C(100)'''$ configuration corresponds to experimental spherical nanometric precipitates[4] with fully constrained lattice parameters. The easy nucleation of $C(101)$ and $C(110)$, both in precipitates and epitaxial layers, can be understood just by considering a very efficient interface bonding. In fact, the silicon pattern corresponding to the both these planes displays a very good matching to the Si(111) one (see Fig. 3). This issue stems from the fact that in the CaF$_2$ structure, which originates the β-FeSi$_2$ orthorhombic form,[33] the (111) plane of silicon atoms corresponds to β-FeSi$_2$(101) and (110) silicon planes. Both in cases of fully strained structures, $C(101)$ and $C(110)$, and for partially relaxed interfaces, $E(101)$ and $E(110)$, the formers are higher in energy with respect to the latters. By considering that the interface bonding is nearly the same (see Fig. 3), our results indicate the β-FeSi$_2$(101) relationship is preferred, in agreement with the STM investigations.[17,23]

B. Electronic properties

The electronic structure of β-FeSi$_2$ with fully relaxed structural parameters ($\widetilde{B}$), calculated along the high-symmetry directions of the base-centered orthorhombic Brillouin zone, is shown in Fig. 1. It is exactly the same as the one displayed in Ref. 13, where a complete discussion on its features was reported. Here we display it just for comparison to the strained structures. The fundamental band gap is found to be 0.62 eV, corresponding to an indirect transition between the valence band maximum (VBM) at the Y point and the conduction band minimum (CBM) situated along the Γ-Z direction, approximately at $0.6\times(\Gamma$-$Z)$. In the following we conventionally call Λ^* the point along the Γ-Z direction where the CBM or VBM occurs. The direct transition located at Y is 0.66 eV. The gap size is some 30% smaller than the experimental one: such an underestimation is within the range usually observed for density-functional results on

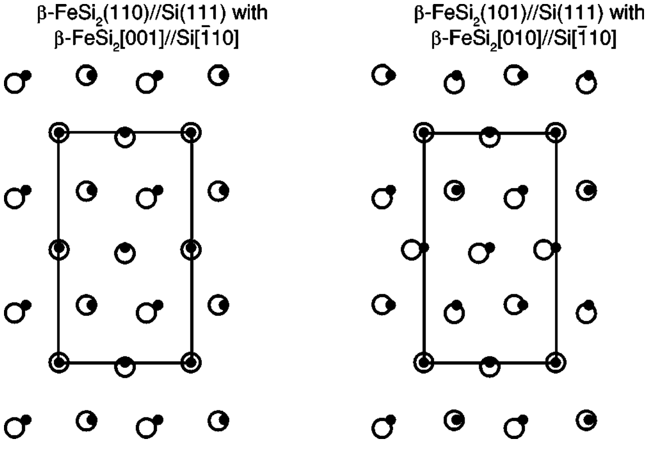

FIG. 3. Top view of the atomic matching at β-FeSi$_2$(110) and (101)//Si(111) for the $C(101)$ and $C(110)$ configurations. The open and solid circles correspond to the Si atoms in β-FeSi$_2$ and in the silicon substrate, respectively.

TABLE III. Eigenvalues (eV) of the valence-band maxima (VBM) and the conduction-band minima (CBM) for some β-FeSi$_2$ structures.

	B			$\overline{B}$			$\tilde{B}$			$E(101)$			$E(110)$		
	Γ	Λ*	Y	Γ	Λ*	Y	Γ	Λ*	Y	Γ	Λ*	Y	Γ	Λ*	Y
VBM	−0.28	−0.10	0.00	−0.23	−0.10	0.00	−0.22	−0.10	0.00	−0.22	−0.08	0.00	−0.25	−0.10	0.00
CBM	0.68	0.64	0.71	0.66	0.63	0.68	0.64	0.62	0.66	0.76	0.72	0.80	0.76	0.71	0.75

	$E(100)$			$E(100)'$			$E(001)$			$E(010)$			$E(010)'$		
	Γ	Λ*	Y	Γ	Λ*	Y	Γ	Λ*	Y	Γ	Λ*	Y	Γ	Λ*	Y
VBM	−0.17	−0.06	0.00	−0.22	−0.08	0.00	−0.15	−0.06	0.00	−0.25	−0.10	0.00	−0.34	−0.15	0.00
CBM	0.64	0.63	0.67	0.65	0.63	0.66	0.60	0.58	0.66	0.63	0.60	0.60	0.83	0.72	0.79

band-gap energies. Still, the energy difference between the direct and indirect transitions (Y-Y and $Y-\Lambda^*$) is quantitatively meaningful, and turns out to be 0.05 eV, in a good agreement with the experimental data.[5]

The band structures for the crystals B, $\overline{B}$, and $\tilde{B}$ are essentially the same. We note that the optimization of the structural parameters for the bulk leads only to a small reduction of the energy gaps (see Table III). The strained structures $E(101)$, $E(110)$, $E(100)$, $E(100)'$, $E(001)$, $E(010)$, and $E(010)'$, which correspond to epitaxial layers with commensurate (reduced strain) interfaces, have almost the same gap shape as in case of the bulk. The corresponding eigenvalues of the band maxima and minima are also given in Table III for the sake of comparison to possible experimental shifts. Conventionally, the valence-band maximum at the Y point is taken to be zero on the energy scale. All these strained structures are characterized by moderate deformations of the lattice constants (one side was changed by about 2% whereas the others by 1% or even less than 1%; see Table II) which do not lead to crucial changes in the band structure of β-FeSi$_2$. One can just observe some (~0.1 eV) increase or decrease of the fundamental gap.

The corresponding band diagrams for the rather strained cases, $C(100)''$, $C(100)'''$, $C(101)$, and $C(110)$, are reported in Figs. 4(a), 4(b), 4(c), and 4(d), respectively. Here one can see major changes in the band dispersion with respect to Fig. 1. In particular, the $C(100)''$ structure [see Fig. 4(a)] provides no changes in the gap nature, but a very flat dispersion of the lowest conduction band and highest valence band. This issue can be understood in terms of the expansion of the b and c sides (see Table II), which in turn generates an increase in all the first-neighor distances (not reported here). In contrast to the case of $C(100)''$, dispersion of the bands nearby the gap for $C(100)'''$ is strongly increased [see Fig. 4(b)]. By considering the lattice parameters in Table II this seems to be caused by a decrease in the b and c sides, which provides a reduction for all the Fe-Si bond lengths. Since the VBM is located at Λ^*, where p-type contributions are neg-

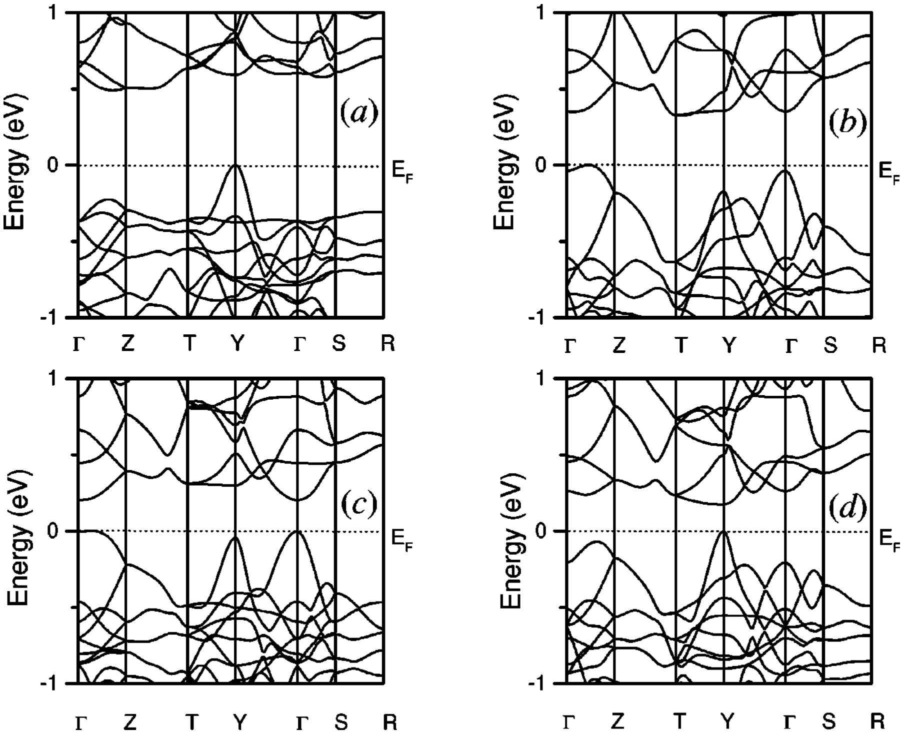

FIG. 4. Band structure for the following configurations: (a) $C(100)''$, (b) $C(100)'''$, (c) $C(101)$, and (d) $C(110)$ (see Table II).

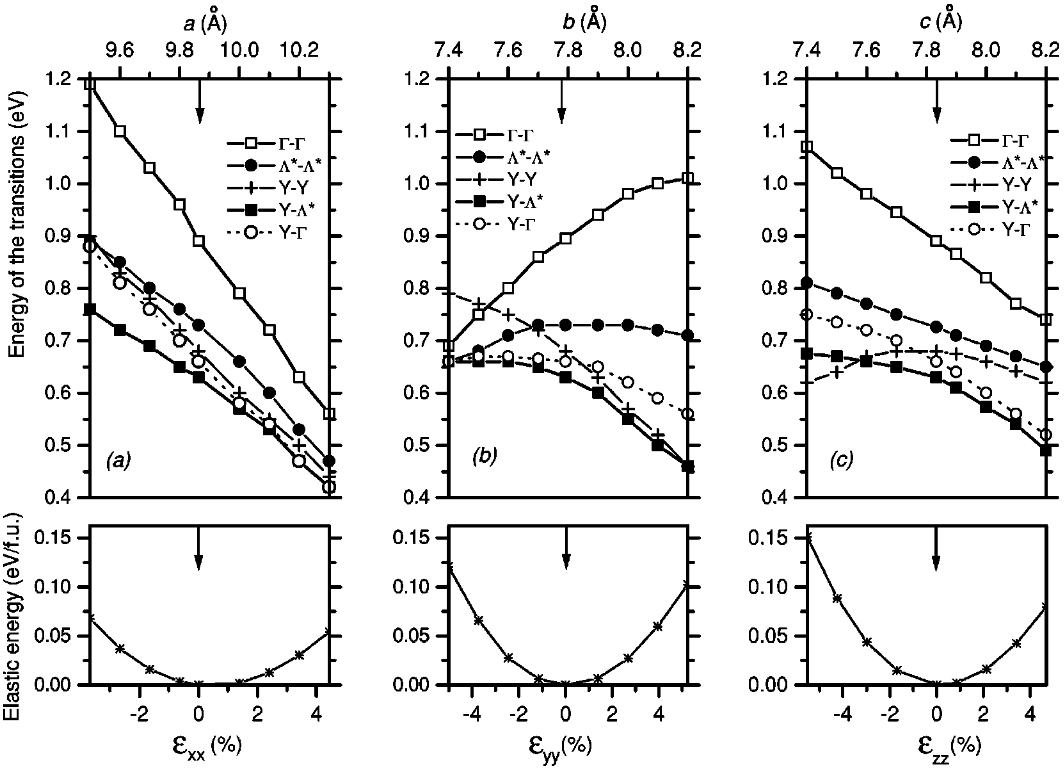

FIG. 5. Variations of some selected gaps (in eV) and corresponding elastic energy (eV/$f.u.$) with uniaxial strain ε (%) for *a* (a), *b* (b), and *c* (c) sides. The corresponding values (Å) of the lattice parameters are in the top scale, and the arrows indicate the bulk experimental values.

ligible, optical transitions to the conduction bands (*d* in character) are predicted to be dipole forbidden, as discussed in Refs. 6 and 13.

While it is experimentally difficult to distinguish β-FeSi$_2$(101) from (110)//Si(111) on structural grounds, due to the large similarity in the *b* and *c* sides, the dispersion of the bands near the energy gap is different for $C(101)$ and $C(110)$; see Figs. 4(c) and 4(d), respectively. In the case of β-FeSi$_2$(101)//Si(111) the gap narrows at Λ^*, whereas for β-FeSi$_2$(110)//Si(111) it shrinks at *Y*. There is a common tendency to change the nature of the gap from indirect to direct, and to close the band gap with respect to the bulk case. Actually, for $C(101)$ the VBM occurs at the Λ^* point, but the energy difference between Λ^* and Γ in the valence band is less than 4 meV. Even if an actual direct transition would be possible at any point close to Γ, the oscillator strength between two bands with mainly the same *d* character would be negligible.[6,13] The band structure of $C(110)$, conversely, is characterized by a direct transition at the *Y* point, where the contribution of *p*-states in the VBM is much larger and promising.[6,13] The same band behavior for the two cases was found in Ref. 9, but there is no quantitative analogy in the two calculations due to a lack of structural optimization in the latter. Since the *b* and *c* sides are alternatively expanded and contracted, no simple interpretation comes from the analysis of the bond lengths and bond angle distributions for the two cases.

C. Uniaxial rigid strain

In order to give an interpretation for the different gap nature between the $C(101)$ and $C(110)$ configurations, calculations for a uniaxial rigid lattice deformation have been performed. We varied one of the lattice constants up to $\pm 5\%$ with respect to the experimental value, keeping the other sides invariable, and relaxing the atomic positions. The dependence of selected band-gap values on the uniaxial strain of the *a*, *b*, and *c*, sides and the corresponding differences in total energy, are shown on Fig. 5. We note that for the *a* side [Fig. 5(a)] a very regular behavior for both direct and indirect transitions is obtained: the gaps open with lattice constant reduction, as occurs for bonding-antibonding gaps in many materials. A complex band-gap behavior was found by changing the *b* and *c* sides [see Figs. 5(b) and 5(c)], particularly for direct transitions in Γ and Λ^*, by varying *b*, and in *Y*, by decreasing *c*. For $c < 7.6$ Å ($\varepsilon_{zz} < -3\%$) the direct transition at the *Y* point becomes lower than any other one: we expect that by decreasing *c* and increasing *b* the fundamental band gap will be at *Y*, as found for the C(110) configuration. If the *b* side is decreased the values for the Y-Γ and Y-Λ^* transitions are very close, while the Y-Y transition is increased and the lowest gap is nearby Γ, as happens in $C(101)$. The elastic energy dependence on the rigid uniaxial side deformation is characterized by a flat behavior for small strains, especially for *a*. This finding can also explain some differences in the optimized lattice constants for the bulk structure present in literature (see Refs. 12 and 13, for instance).

Despite the fact that the *b* (7.791 Å) and *c* (7.833 Å) sides are very close in size, band gaps corresponding to a rigid change of either one or the other do display a sizable anisotropy. Actually, the Jahn-Teller distortion of the cubic cage of Si atoms around the Fe site, which leads to β-FeSi$_2$ formation starting from the CaF$_2$ structure,[33] provides a symmetry breaking for the y and z coordinates. Even if it is not straightforward to see a relevant structural anisotropy both in bond lengths and in bond-angle distributions, some optical measurements, such as infrared absorption,[34] do indicate the anisotropy in the b and c sides.

V. CONCLUSIONS

β-FeSi$_2$ displays a large lattice misfit with Si(111): depending on the epitaxial relationship it can be as large as 5%. Moreover, the different symmetry of the two structures is commonly believed to be an additional feature preventing a good epitaxy of iron disilicide on silicon. However, the growth of nanometric dots with comparable strain energies [like Ge on Si(001)] is now within the present technology, and in this paper we point out that the two most common epitaxial relationships on and in silicon, β-FeSi$_2$(101) and (110)//Si(111), compensate for the high strain energy with a very good atomic matching at the interface. Therefore, in relation to very recent experiments of nanometric dots in silicon[4] and future developments, we calculated the band structure corresponding to the coherent and commensurate interfaces with Si(111). We obtained that only one configuration β-FeSi$_2$(110)//Si(111) does provide an interesting change in the gap nature, from indirect to direct. Another important result of our calculations is an unexpected anisotropy of the band structure of iron disilicide due to the rigid uniaxial deformations of the almost equal b and c sides.

ACKNOWLEDGMENTS

The authors would like to thank J. Hafner, G. Kresse, and V. E. Borisenko for kind assistance on the VASP code, and for critical comments on this manuscript, respectively. This work was partially supported by Confinaziamento 40% 1998 of the Italian Ministry of University and Research (Grant No. 9802154837) and by UNESCO-ROSTE.

---

[1] H. Lange, Phys. Status Solidi B **201**, 3 (1997); *Semiconducting Silicides*, edited by V. E. Borisenko (Springer, Berlin, 2000).

[2] M. C. Bost and J. E. Mahan, J. Appl. Phys. **58**, 2696 (1985); C. A. Dimitriadis, J. H. Werner, S. Logothetidis, M. Stutzmann, J. Weber, and R. Nesper, *ibid.* **68**, 1726 (1990); D. J. Oostra, C. W. T. Bulle-Lieuwma, D. E. W. Vanderhoubt, and J. C. Jans, *ibid.* **74**, 4347 (1993); K. Lefki, P. Muret, N. Cherief, and R. C. Cinti, *ibid.* **69**, 352 (1991).

[3] D. N. Leong, M. A. Harry, K. J. Reeson, and K. P. Homewood, Nature (London) **387**, 686 (1997).

[4] C. Spinella, S. Coffa, C. Bongiorno, S. Pannitteri, and M. G. Grimaldi, Appl. Phys. Lett. **76**, 173 (2000).

[5] C. Giannini, S. Lagomarsino, F. Scarinic, and P. Castrucci, Phys. Rev. B **45**, 8822 (1992); K. Radermacher, R. Carius, and S. Mantl, Nucl. Instrum. Methods Phys. Res. B **84**, 163 (1994); H. Lange, W. Henrion, B. Selle, G.-U. Reinsperger, G. Oertel, and H. von Känel, Appl. Surf. Sci. **102**, 169 (1996).

[6] A. B. Filonov, D. B. Migas, V. L. Shaposhnikov, N. N. Dorozhkin, G. V. Petrov, V. E. Borisenko, W. Henrion, and H. Lange, J. Appl. Phys. **79**, 7708 (1996); A. B. Filonov, D. B. Migas, V. L. Shaposhnikov, V. E. Borisenko, W. Henrion, M. Rebien, P. Stauss, H. Lange, and G. Behr, *ibid.* **79**, 7708 (1998).

[7] N. E. Christensen, Phys. Rev. B **42**, 7148 (1990); N. E. Christensen, I. Wenneker, A. Svane, and M. Fanciulli, Phys. Status Solidi B **198**, 23 (1996).

[8] J. van Ek, P. E. A. Turchi, and P. A. Sterne, Phys. Rev. B **54**, 7897 (1996); V. N. Antonov, O. Jepsen, W. Henrion, M. Rebien, P. Stauss, and H. Lange, *ibid.* **57**, 8934 (1998).

[9] L. Miglio and V. Meregalli, J. Vac. Sci. Technol. B **16**, 1604 (1998).

[10] L. Miglio, V. Meregalli, and O. Jepsen, Appl. Phys. Lett. **75**, 385 (1999).

[11] R. Eppenga, J. Appl. Phys. **68**, 3027 (1990).

[12] S. J. Clark, H. M. Al-Allak, S. Brand, and R. A. Abram, Phys. Rev. B **58**, 10 389 (1998).

[13] E. G. Moroni, W. Wolf, J. Hafner, and R. Podloucky, Phys. Rev. B **59**, 12 860 (1999).

[14] S. Eisebitt, J. E. Rubensson, M. Nicodemus, T. Böske, S. Blügel, W. Eberhardt, K. Radermacher, S. Mantl, and G. Bihlmayer, Phys. Rev. B **50**, 18 330 (1994).

[15] P. Y. Dusausoy, J. Protas, R. Wandji, and B. Roques, Acta Crystallogr., Sect. B: Struct. Crystallogr. Cryst. Chem. **27**, 1209 (1971).

[16] N. Jedrecy, Y. Zheng, A. Waldhauer, M. Sauvage-Simkin, and R. Pinchaux, Phys. Rev. B **48**, 8801 (1993).

[17] W. Raunau, H. Niehus, T. Schilling, and G. Comsa, Surf. Sci. **286**, 203 (1993).

[18] J. M. Gay, P. Stocker, and F. Rethore, J. Appl. Phys. **73**, 8169 (1993).

[19] A. L. Vazquez de Parga, J. de la Figuera, J. E. Pieto, C. Ocal, and R. Miranda, Appl. Phys. A: Solids Surf. **57**, 477 (1993).

[20] J. Derrien, J. Chevrier, V. Le Thanh, and J. E. Mahan, Appl. Surf. Sci. **56–58,** 382 (1992).

[21] J. E. Mahan, V. Le Thanh, J. Chevrier, I. Berbezier, J. Derrien, and R. G. Long, J. Appl. Phys. **74**, 1747 (1993).

[22] A. Rizzi, B. N. E. Rosen, D. Freundt, Ch. Dieker, H. Luth, and D. Gerthsen, Phys. Rev. B **51**, 17 780 (1995).

[23] H. Sirringhaus, N. Onda, E. Muller-Gubler, R. Stalder, and H. von Känel, Phys. Rev. B **47**, 10 567 (1993).

[24] J. Tavares, H. Bender, and K. Maex, Thin Solid Films **227**, 90 (1996).

[25] D. J. Oostra, D. E. W. Vandenhoubt, C. W. T. Bulle-Lieuwma, and E. P. Naburgh, Appl. Phys. Lett. **59**, 1737 (1991).

[26] M. Sauvage-Simkin, N. Jedrecy, A. Waldhauer, and R. Pinchaux, Physica B **198**, 48 (1994).

[27] D. Gerthsen, K. Radermacher, Ch. Dieker, and S. Mantl, J. Appl. Phys. **71**, 3788 (1992); K. Radermacher, S. Mantl, D. Gerthsen, Ch. Dieker, and H. Luth, Nucl. Instrum. Methods Phys. Res. B **80/81**, 831 (1993).

[28] G. Kresse and J. Hafner, Phys. Rev. B **49**, 14 251 (1994); G. Kresse and J. Futhmüller, Comput. Mater. Sci. **6**, 15 (1996); Phys. Rev. B **54**, 11 169 (1996).

[29] J. Perdew and Y. Wang, Phys. Rev. B **45**, 13 244 (1992).

[30] D. Vanderbilt, Phys. Rev. B **41**, 7892 (1990); G. Kresse and J. Hafner, J. Phys.: Condens. Matter **6**, 8245 (1994).

[31] P. Blöchl, O. Jepsen, and O. K. Andersen, Phys. Rev. B **49**, 16 223 (1994).

[32] H. J. Monkhorst and J. D. Pack, Phys. Rev. B **13**, 5188 (1976).

[33] F. Tavazza, V. Meregalli, L. Miglio, and M. Celino, Phys. Rev. B **59**, 3480 (1999).

[34] G. Guizzetti, F. Marabelli, M. Patrini, P. Pellegrino, B. Pivac, L. Miglio, V. Meregalli, H. Lange, W. Henrion, and V. Tomm, Phys. Rev. B **55**, 14 290 (1997).